Molecular Crystals and Liquid Crystals
Publication details, including instructions for authors and subscription information:
http://www.tandfonline.com/loi/gmcl16

Photoinjection of Charge Carriers into 1,3,5-Trintrobenzene Single Crystal

Andrzej Miniewicz [a] & Digby F. Williams [a b]
[a] Institute of Organic and Physical Chemistry, Technical University of Wroclaw, 50-370, Wroclaw, Poland
[b] Division of Chemistry, National Research Council of Canada, Ottawa, KIA OR6
Version of record first published: 20 Apr 2011.

To cite this article: Andrzej Miniewicz & Digby F. Williams (1984): Photoinjection of Charge Carriers into 1,3,5-Trintrobenzene Single Crystal, Molecular Crystals and Liquid Crystals, 106:1-2, 1-19

To link to this article: http://dx.doi.org/10.1080/00268948408080175

Mol. Cryst. Liq. Cryst., 1984, Vol. 106, pp. 1–19
0026-8941/84/1062–0001/$18.50/0

Printed in the United States of America

Photoinjection of Charge Carriers into 1,3,5-Trinitrobenzene Single Crystal

ANDRZEJ MINIEWICZ and DIGBY F. WILLIAMS†

Institute of Organic and Physical Chemistry, Technical University of Wroclaw, 50-370 Wroclaw, Poland

(*Received October 17, 1983*)

The DC photoresponse has been measured for 1,3,5 trinitrobenzene crystals as a function of excitation wavelength and applied field. Photoelectrodes used included a-Se, CdTe, Te, ZnO and gold. Current–voltage characteristics of all systems barring Se–TNB were similar. The origin and nature of the photocurrent peaks at 480–450 nm and the following increase (decrease) of the photocurrent, common to all systems independent of electrode material is discussed and analysed in terms of a two component process, injection and optical detrapping. From the analysis an energy diagram of the systems together with probable photoinjection mechanisms are obtained.

I. INTRODUCTION

In our recent paper[1] we have reported on charge carrier drift mobility measurements in 1,3,5-trinitrobenzene (TNB) single crystal. As TNB crystals are non-photoconducting, we sensitized their surfaces with evaporated thin layers of amorphous selenium or cadmium telluride in order to photo-inject electrons or holes.

Pulsed photoconductivity experiments could not however, supply information about the energetic structure of the semiconductor-insulator interface and no clear distinction could be made between various possible photoinjection processes. To this end, direct measurements of the action spectrum for photocarrier production have been carried out.

The conventional dc photoconductivity technique was employed to examine the photoinjection efficiency of electrons and holes into TNB

†Division of Chemistry, National Research Council of Canada, Ottawa, K1A OR6.

as a function of excitation wavelength and applied voltage. Results of experiments performed with electrodes other than Se and CdTe, namely Te, ZnO and Au are also presented and discussed.

Selenium, cadmium telluride and tellurium have been used previously to sensitize various insulators such as crystalline sulfur,[2,3] poly(*N*-vinyl-carbazole),[4,5] poly/*N*-vinyl-carbazole/: trinitrofluorenone 1 : 1 charge transfer complex,[6] trinitrofluorenone,[7] etc. However, up to date no general theory describing features of photoinjection of charge carriers from a semiconductor into a narrow band, wide gap insulator has been put forward.

II. EXPERIMENTAL

1,3,5-trinitrobenzene single crystals were obtained as described in [1]. The platelets, usually 0.3–0.8 mm thick and 0.5 cm^2 in area, were polished with benzene. All electrodes, except ZnO, were vacuum deposited (at about 10^{-2} Pa) on the crystalline substrate held slightly above room temperature. Thin electrode layers of amorphous Se (0.1 μm), polycrystalline films of CdTe,[8] amorphous layers of Te and 150–200 Å layers of Au were prepared. Thin insulating layers of ZnO were deposited by an RF sputtering technique. The visible transparencies of these films were 50–80% as measured with a Cary spectrophotometer. The dc photocurrent action spectra have been measured using a "sandwich" type configuration. Samples were mounted in a thermostated chamber equipt with a quartz window, and they were held by a gentle pressure between conducting glass front electrode and a rear silver paste electrode. If not specified otherwise, the semiconducting layers were illuminated through the transparent conducting glass to which the bias voltages were applied. A 2.5 kW Hanovia Xe arc with a water filter followed by a Chromatix 1 m grating monochromator served as a source of monochromatic light. Photocurrents I^+ and I^- (with positively and negatively biased front electrode respectively), were measured with a Keithley 440 Digital Picoammeter driving a chart recorder. Action spectra of the photocurrent were taken using two procedures: (i) continuous recording of the photocurrent with slow (20 nm per minute) scanning of excitation light wavelength; and (ii) step by step recording, i.e. setting a wavelength on the monochromator and recording the sample's response prior to and after opening the shutter. Photocurrents are defined as differences between photo- and dark currents measured with the front electrode biased negatively (electron photocurrent $I^e_{ph} = I^-_{ph} - I^-_d$) and

positively (hole photocurrent $I_{ph}^{h} = I_{ph}^{+} - I_{d}^{+}$). To be valid these definitions require that all charge carriers are produced in the electrode layer deposited on the sample. Separate experiments were performed to confirm this assumption. Indeed, after the photosensitive electrode has been removed from TNB front surface no photocurrents could be observed. We should point out that I_{ph}^{e} and I_{ph}^{h} measured by the step-by-step procedure represent steady-state values of photocurrents which were usually reached in 1–3 minutes after opening the shutter.

In order to correct the photocurrent action spectra to equal intensity of excitation light, photon fluxes for each wavelength were determined by a 8330 Å Hewlett Packard Radiant Flux meter and the light intensity dependences were checked using a rotary neutral density filter. All measurements were carried out at room temperature.

III. RESULTS

A. Se–TNB system

Photoconductivity experiments performed on the Se–TNB system indicate that only electrons can be photoinjected into the TNB bulk i.e. no photocurrent has been observed when the illuminated Se electrode was positively biased. Essentially no measurable dark injection occurred: dark currents I_{d}^{+} and I_{d}^{-} were both of the same order, i.e. below 5×10^{-14}A with applied fields F of 2.7×10^{4} V/cm. The kinetic behaviour of the photoinjection process as seen in the dc experiment was reflected by a sharp current spike (duration less than 1 sec) just after opening of the shutter, followed by a slow decay to the stationary value within 1–2 minutes. The steady-state value of electron photocurrent I_{ph}^{e} was usually two times smaller than that at the spike.

The photocurrent–electric field characteristics taken at various wavelengths of excitation light are shown in Figure 1. As is clearly seen, a sharp increase of the photocurrent occurs above a critical electric field F_c, F_c being also a weak function of wavelength. A closer inspection shows that this critical field increases with increasing photon energy and that such a critical field cannot be extracted from the I-F plot for photons with energy smaller than ca. 2.2 eV.

For the purpose of this paper we define a quantity η_{e}^{Se-TNB} related to quantum photogeneration efficiency η_{e}^{Se} in a-Se[9] but describing the efficiency of photogeneration process in the whole Se–TNB system. Let η_{e}^{Se-TNB} be the quantum efficiency of electron collection; i.e. the number of carriers reaching the rear electrode after absorption of a

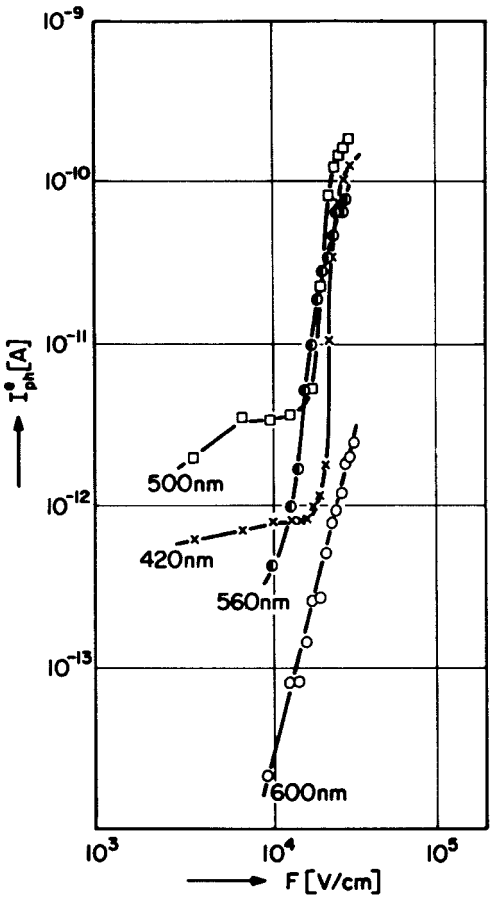

FIGURE 1 Field dependences of the steady-state electron photocurrent flowing through a Se–TNB structure for different wavelengths of incident radiation. Currents are corrected for equal density of incident photons.

single photon in Se layer, then one can expect a direct correlation between η_e^{Se-TNB} and η_e^{Se}, however, due to interface phenomena and transport properties of TNB such a correlation will be distorted. In order to compare wavelength dependences of both parameters we have plotted them in Figure 2. The values of η_e^{Se} have been taken from,[10] whereas values of η_e^{Se-TNB} have been calculated from measured photocurrent action spectrum for Se–TNB system. Both parameters were taken at $F = 2.74 \times 10^4$ V/cm and the η^{Se-TNB} was normalized to equal density of incident photons $I_0 = 10^{13}$ photons/cm^2.s and cor-

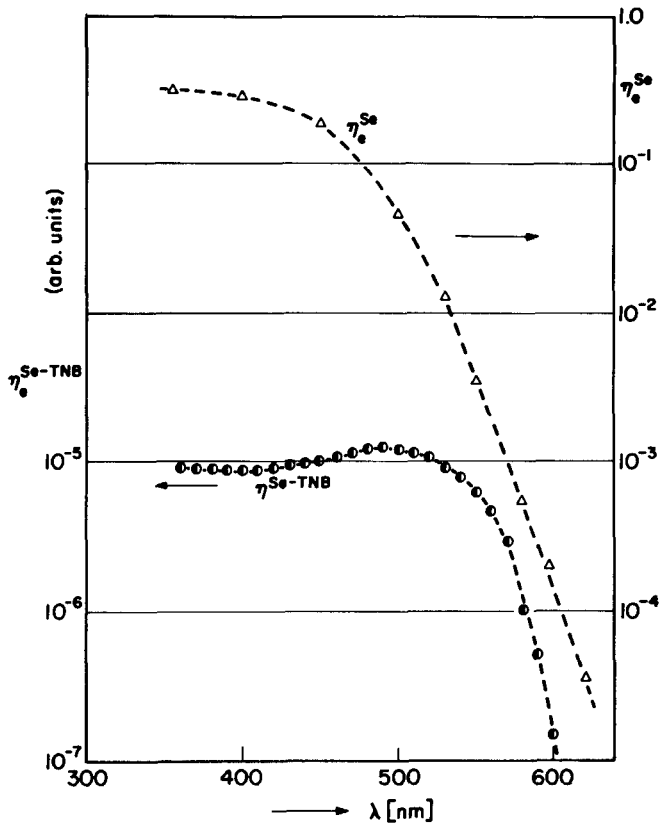

FIGURE 2 Wavelength dependencies of collection efficiency of electrons η_e^{Se-TNB} in Se–TNB structure (η_e^{Se-TNB} has been corrected for equal density of incident photons ca. 10^{13} photons/sec cm^2 and for reflection losses in a-Se) and quantum efficiency of electrons η_e^{Se} in a-Se taken from.[10] Both efficiencies were taken at the electric field equal to 2.74×10^4 V cm.

rected with respect to reflectivity spectrum of a-Se.[11] To better visualize the differences between η_e^{Se} and η_e^{Se-TNB} in the studied wavelength range we introduce the parameter $G(\lambda)$ defined by the equation:

$$\eta_e^{Se-TNB}(\lambda) = G(\lambda) \cdot \eta_e^{Se}(\lambda) \qquad (1)$$

The wavelength dependence of $G(\lambda)$ shown in Figure 3 is to some extent peculiar. One can distinguish three characteristic regions: 340–410 nm where $G(\lambda)$ is constant and of order 3×10^{-5}; 410–570

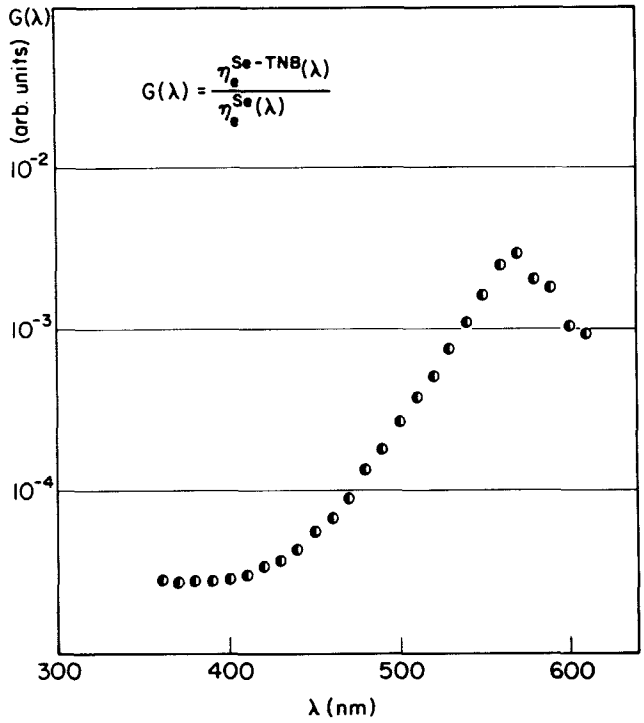

FIGURE 3 Wavelength dependence of the parameter $G(\lambda)$ defined as: $G(\lambda) = \eta_e^{Se-TNB}(\lambda) \cdot (\eta_e^{Se}(\lambda))^{-1}$.

nm where $G(\lambda)$ monotonically increases reaching at the maximum ca. 3×10^{-3} and 570–620 nm where $G(\lambda)$ decreases. Explanation of such a behaviour will be attempted in Section III.

B. CdTe–TNB system

In CdTe–TNB structures both electron and hole photocurrents were measured probably due to a specific matching of energetic levels of CdTe and TNB. Dark current and photocurrent versus voltage characteristics shown in Figure 4. Contrary to Se–TNB structures, both (+) and (−) dark currents are not small, ranging up to ca. 2×10^{-11} A. Both follow a quadratic voltage dependence for lower voltages and $I\text{-}U^{3.59}$ for higher voltages with I_d^h being slightly higher than I_d^e. Electron and hole photocurrents are less than an order of magnitude smaller than respective dark currents prompting us to regard them as

photoenhanced currents. The relation $I_d^h > I_d^e$ is maintained and even strengthened for photoenhanced currents at least in the spectral region where both could be measured.

Spectral characteristics of photoenhanced hole and electron currents, corrected for reflection losses in the CdTe film[12] are shown in Figure 5. As is clearly seen, the photoenhanced hole current vanishes completely for wavelengths shorter than ca. 430 nm, whereas the photoenhanced electron current is only reduced in this spectral region and rises again with further decrease of excitation wavelength.

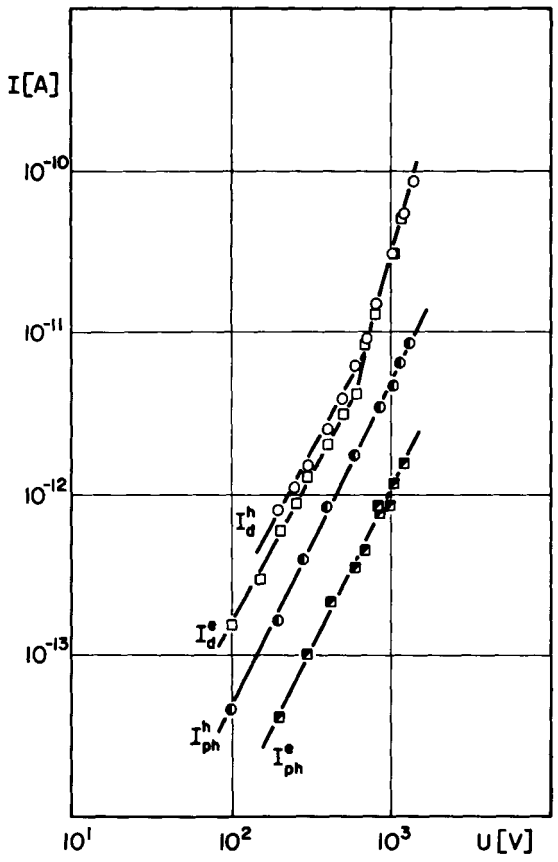

FIGURE 4 Dark current and photocurrent versus voltage characteristics in CdTe–TNB structure. Note that photocurrents recorded as a difference between sample response under illumination and in the darkness are smaller than dark currents.

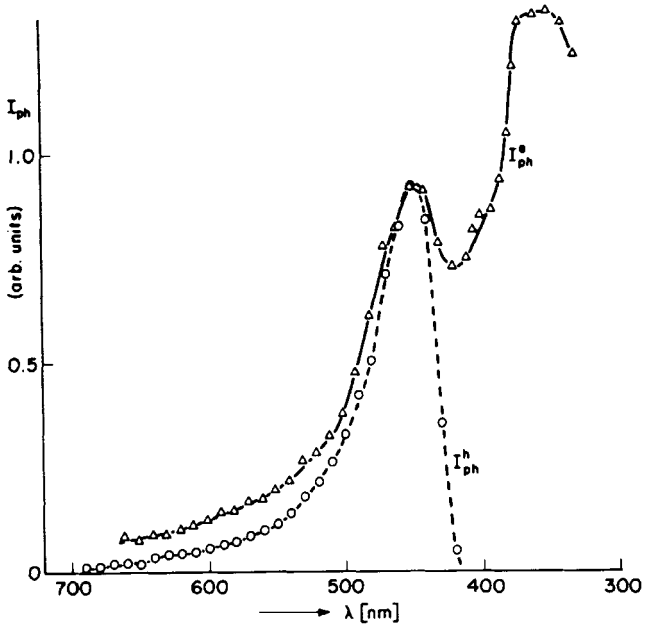

FIGURE 5 Spectral characteristics of photoenhanced hole I^h_{ph} and electron I^e_{ph} currents in CdTe–TNB structure. Correction have been made due to reflection losses in CdTe. Both currents has been normalized to equal density of incident photons ca. 10^{13} photons/sec cm^2 and to unity at 460 nm.

C. Te–TNB system

The properties of the Te–TNB structure resemble to some extent properties of CdTe–TNB rather than those of Se–TNB. In this case a pronounced asymmetry between (+) and (−) dark currents as well as photocurrents exists. The current–voltage characteristics shown in Figure 6 indicate that the photoenhanced electron current is more than two orders of magnitude larger than the photoenhanced hole current, the same being true for dark currents. However, due to the small values of photoenhanced hole currents even for large applied fields we did not record any spectra. Thus only an electron photocurrent action spectrum corrected for the reflection[11] is shown in Figure 7. It is noticeable that a small decrease of the photocurrent occurs near 430 nm i.e. approximately in the same region as in CdTe–TNB case.

D. ZnO–TNB system

In spite of RF sputtered thin layers of insulating ZnO being almost transparent in the 700–430 nm region, photocurrents were observed in

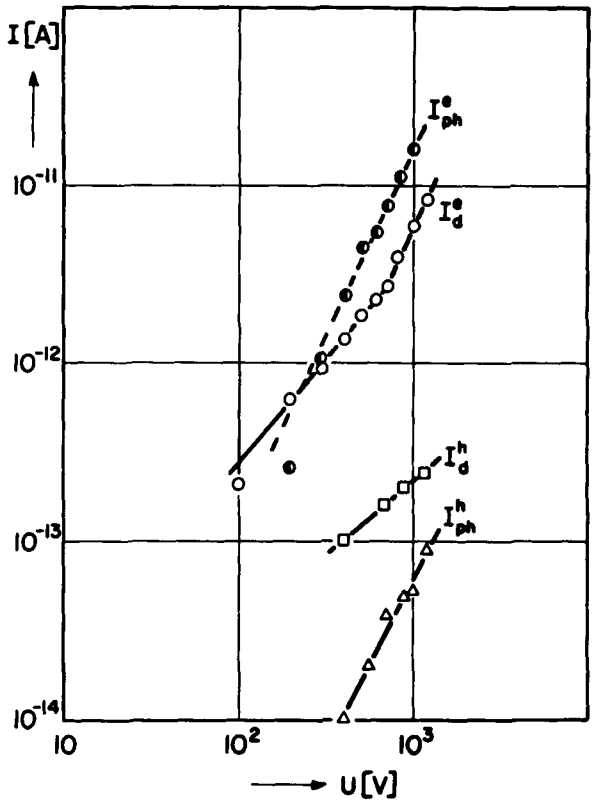

FIGURE 6 Dark and photocurrent versus voltage characteristics in Te–TNB structure.

the system. We have found that holes only could be photoinjected into TNB bulk. Dark hole and electron currents were both found to be below the sensitivity range of our electrometer. As is seen in Figure 8, hole photocurrents follow a quadratic voltage dependence.

The photoconductivity spectrum normalized to equal density of incident photons shown in Figure 9 reveals features similar to those encountered in the case of photoenhanced hole current in CdTe–TNB structure i.e. the pronounced decrease of current to zero value for wavelengths shorter than ca. 430 nm.

E. Au–TNB system

In addition to the sensitizers mentioned above, we have attempted to inject charge carriers into TNB from a gold electrode. No dark

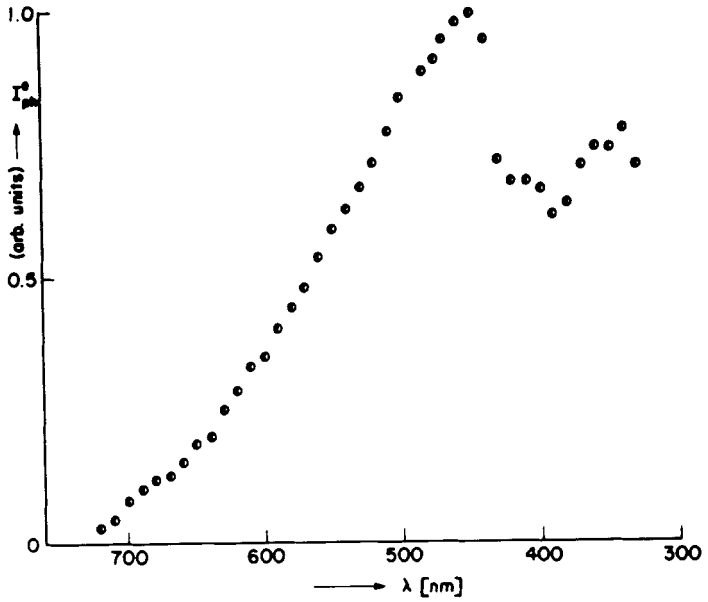

FIGURE 7 Photoenhanced hole current action spectrum in Te–TNB structure. Correction has been made for reflection losses in Te and the current is normalized to equal density of incident photons ca. 10^{13} photons/sec cm^2.

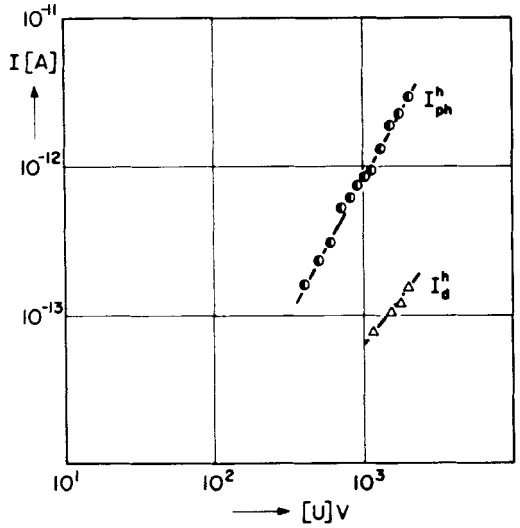

FIGURE 8 Dark and photocurrent versus voltage characteristics in ZnO–TNB structure.

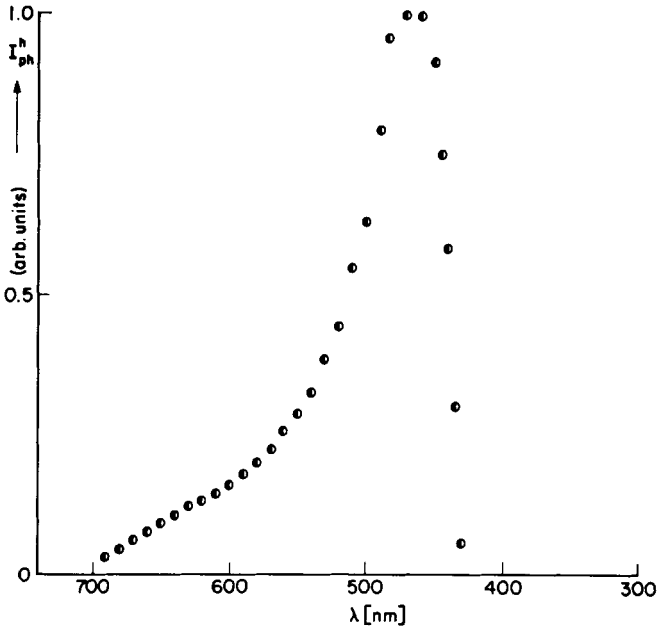

FIGURE 9 Photoenhanced hole current action spectrum in ZnO–TNB structure. The current is normalized to equal density of incident photons ca. 10^{13} photons/sec cm^2.

injection for both (+) and (−) polarizations was detected, though experiments with light showed that a small hole photocurrent has emerged above the noise level.

F. Summary of results

Considering all the experimental data obtained for various semiconductor-dielectric structures, TNB being the dielectric, some questions arise with respect to the development of a general explanation. The crucial question is that of the origin and nature of the peaks of photocurrents in the region 480–450 nm followed by weaker or stronger decrease of the photocurrent. This feature is common to all measured action spectra, though no correspondence could be found with absorption spectra of the electrode materials used. It is also hard to understand why the photocurrent vanishes for wavelengths shorter than ca. 415 nm in the case of CdTe–TNB and ZnO–TNB structures.

Since the current–voltage characteristics in the case of Se–TNB are different from those for other systems studied, it is natural to assume that the mechanism of photoinjection is also different. Other

differences between the systems studied are likely to arise from different positioning of energetic levels of the semiconductors with respect to those of TNB, thus it can be hoped that information on positions of bands in TNB may be derived from these data.

III. DISCUSSION

The analysis of photogeneration mechanisms active in our samples can be performed considering the following model. Let us assume that the process of charge carrier injection into the insulator bulk from its sensitized surface is a sum of two processes: (i) a photoinjection of hot or thermalized charge carriers photogenerated in the semiconductor after light absorption and subsequently transported to and over the interface potential barrier with the help of externally applied electric field; and (ii) an optical release of carriers, trapped earlier in the bulk of insulator, by the remaining part of incident light which has not been absorbed in the thin film of the semiconductor.

Such an apparently oversimplified model seems to explain most of our experimental results. A strong support for this interpretation comes from the fact that, regardless of the electrode used, an apparent decrease of photocurrent occurs at a wavelength corresponding to the absorption threshold for crystalline TNB (420 nm). Above the threshold the light cannot penetrate into TNB deeper than ca. 10^{-5} cm, and hence the current increment coming from the optical detrapping process becomes negligible. In an extreme situation, when only the process [ii] dominates, one can expect the photocurrent to decrease down to zero for wavelengths shorter than ca. 420 nm. This may be the case for hole photocurrents in CdTe–TNB and ZnO–TNB structures. In other investigated systems both processes [i] and [ii] give contributions to overall photocurrent action spectra, though their relative significance is different in each case.

The optical detrapping current, depending on the number of charge carriers released from traps under illumination should be proportional to the intensity of the light entering the crystal as well as to the number of charge carriers occupying traps in its bulk. The former factor is dependent only on the transparency of the deposited semiconductor electrode and on the absorption coefficient of the insulator. The latter factor depends on the efficacy of filling the traps by either dark or light-assisted injection from the electrode and on the energetic and spatial distribution of trapped charge in the bulk.

The optical detrapping current can be evaluated and calculated as a function of exciting light wavelength even if the nature of the exact photodetrapping process is not known. The efficiency of such a process (which can be either of photon-trapped charge carrier or of exciton-trapped charge carrier type) can be described by a parameter. Reimer and Baessler[13] and Godlewski and Kalinowski (GK)[14] have attempted to approach this problem. In the present paper the approach of GK in a modified form will be employed.

Starting from usual basic equations for carrier transport GK introduced an occupation statistics function, $f(E, n_f, I)$ which takes into account simultaneous thermal and optical detrapping, in the form:

$$f(E, n_f, I) = \frac{1}{1 + \frac{N_{\text{eff}}}{n_f}\exp\left(\frac{E}{kT}\right) + \frac{A\chi I}{\nu}} \tag{2}$$

Here E denotes an energy, n_f is the density of free carriers, I is the light intensity at a distance x from the insulator surface, N_{eff} is the effective density of states, ν is the thermal collision factor, χ is the absorption coefficient of the insulator and k and T have their usual meanings. The parameter A can be regarded as an efficiency of the photodetrapping process and describes the number of free carriers released from traps in a unitary volume after absorption of a certain number of photons in this volume. For a spatial and energetic distribution of traps represented by the function $h(E, x)$ the density of trapped carriers $n_t(x)$ can be found from the equation:

$$n_t(x) = \int_0^\infty h(E, x) \cdot f(E, n_f, I)\, dE \tag{3}$$

Using the concept of a demarcation level and neglecting the contribution of diffusion currents together with an assumption of $n_t(x) \gg n_f(x)$ and for an exponential energetic distribution of traps $h(E, x) = H(kT_c)^{-1}\exp(-E/kT_c)$, T_c being the so-called characteristic temperature of the distribution of traps, GK have found an approximate solution for $n_t(x)$ for the case of an inhomogeneous excitation (mostly realized in practice) of the form $I(x) + I_0\exp(-\chi x)$:

$$n_t(x) = \frac{n_f}{N_{\text{eff}}}\frac{H \cdot \pi}{l\sin(\pi/l)}\left[A\chi I_0 \nu^{-1}\exp(-\chi x) + \frac{n_f}{N_{\text{eff}}}\right]^{(l^{-1}-1)} \tag{4}$$

where $l = T_c/T$.

In order to apply this approach i.e. to calculate the wavelength dependence of optical detrapping current increment to the overall measured photocurrent spectra, we have to introduce a wavelength dependence of absorption coefficient (λ). Let us assume the spatial dependence of trap distribution in the following form:

$$h(E, x) = \frac{H}{kT_c} \exp(-E/kT_c) \cdot S_t(x) \tag{5}$$

We shall consider two cases: $S_t(x)$ being equal to 1 (a uniform distribution) and to $\exp(-Bx)$ (an exponential distribution), B being a constant.

Now, substituting $h(E, x)$ into Eq. (3) we obtain:

$$n_t(x, \lambda, I_0) = \frac{n_f}{N_{\text{eff}}} \frac{H \cdot S_t(x) \cdot \pi}{l \sin(\pi/l)} \times \left[\frac{A\chi(\lambda) I_0}{\nu} \exp(-\chi(\lambda)x) + \frac{n_f}{N_{\text{eff}}} \right]^{l^{-1}-1} \tag{6}$$

In order to compute the current arising from photo released charge carriers $I_{\text{opt. det.}}(\lambda)$ one has to calculate how many $N_r(\lambda)$ have been detrapped by light within time interval:

$$I_{\text{opt.det.}}(\lambda) = e \cdot \frac{dN_r(\lambda)}{dt} \tag{7}$$

Here $N_r(\lambda)$ represents a difference between the densities of trapped carriers in the dark and under light of intensity I_0, integrated over the crystal thickness d and multiplied by the electrode area S:

$$N_r(\lambda) = S \cdot \int_0^d [n_t(x, \lambda, 0) - n_t(x, \lambda, I_0)]\, dx \tag{8}$$

Under a properly chosen electric field, most of the photo released charge carriers reach the counter electrode without being retrapped by a deep trap or lost by the recombination; thus the $I_{\text{opt. det.}}(\lambda)$ should reflect the current component associated with the process (ii). Among many constants and parameters used in our calculations the value of A is of great importance and we have to assume it to be wavelength-independent for the lack of the knowledge of details of the optical

detrapping process in that particular case. The estimation of the proper magnitude of A is also important, however its starting value can be estimated by equating the release rates of charge carriers released thermally and by light for a chosen wavelength λ^1 at position x with respect to the electrode:

$$\frac{I_0 \cdot A(\lambda^1)}{\nu} \exp(-\chi(\lambda^1) \cdot x) = \frac{n_f(x)}{N_{\text{eff}}} \tag{9}$$

The absorption coefficient $\chi(\lambda)$ has been taken from a direct measurement of $\chi(\lambda)$ in the single crystal of TNB; the absorption threshold tail has been fitted using Urbach's rule. The trap distribution parameters have been postulated a priori having in mind that only deep traps play a role in the described process and that current–voltage characteristics obtained in the darkness (see CdTe–TNB case) can supply some information about the parameter l (see eq. 6) due to the well known dependence: $I_{\text{SCL}} \sim u^{l+1}$. Other necessary parameters have been chosen as average values typical for most molecular crystals.

The calculations were performed in the spectral region 380–540 nm with $\chi(\lambda)$ for TNB varying from 3.2×10^{-2} cm^{-1} to 3.14×10^5 cm^{-1} respectively. The values of constants were as follows: $n_f = 10^{10}$ cm^{-3}, $N_{\text{eff}} = 10^{21}$ cm^{-3}, $H = 10^{17}$ cm^{-1}, $E = 0.5$ eV, $T_c = 764$ K, $l = 2.59$, $\nu = 10^{13}$ s^{-1}, $I_0 = 10^{13}$ photons cm^{-1}s^{-1}, $d = 0.8$ mm and $F = 1.625 \times 10^4$ V cm^{-1}.

Results of calculations are presented in Figure 10. Calculated spectra, normalized to their maximum values, are compared with photoenhanced current spectrum obtained for the CdTe–TNB system. Except for a small difference in the maximum positions, the shapes of the measured and calculated spectrum (with $A = 6.64 \times 10^{-12}$ cm^3) can be matched almost perfectly. This fact suggest that the described above model can explain the antibatic behaviour of the contribution of the optical detrapping to the photocurrent in the systems studied. Moreover, the knowledge of absorption spectrum and photoenhanced current spectrum may in certain cases be helpful in finding the wavelength dependences of the parameter A (see Reimer *et al.*[13]). In our opinion the effect of light absorption in the semiconductor layer (not considered in our calculations) may be responsible for the shift between the calculated and measured spectrum.

At this point we should stress that most of the presented spectra contain also the second component of the photocurrent due to "real" photoinjection from the electrodes. This process, however, is governed

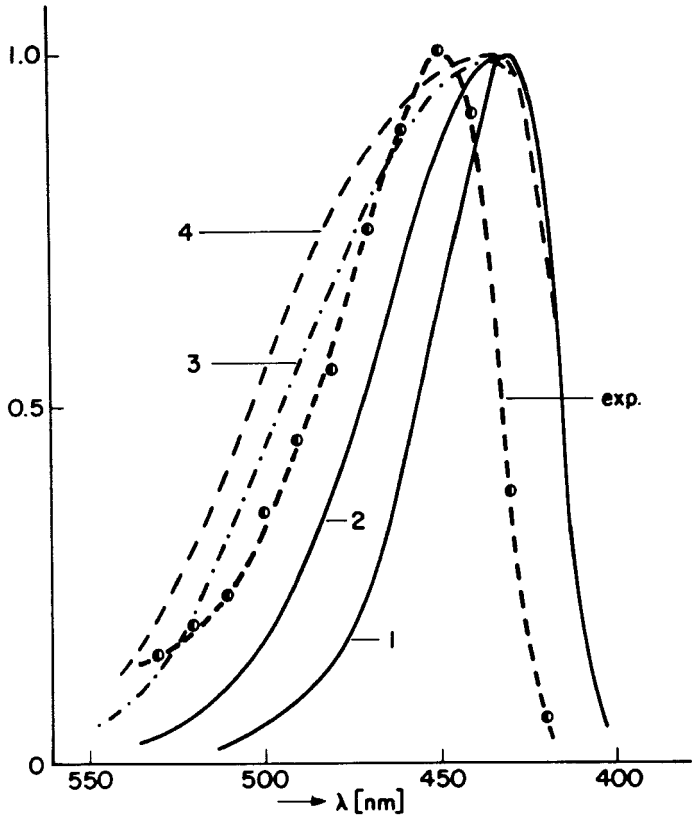

FIGURE 10 Comparison of experimentally obtained photoenhanced hole current action spectrum in CdTe–TNB structure with calculated on the basis of presented model spectra (see text for details). The spectra were normalized to unity at their maximum values. The parameter A is: $6.64 \cdot 10^{-13}$ curve 1; $6.64 \cdot 10^{-12}$ curve 2, $3.32 \cdot 10^{-11}$ curve 3 and $6.64 \cdot 10^{-11}$ curve 4. $S_t(x) = 1$. Changing the B value in reasonable range $S_t(x) = \exp(-Bx)$ small changes in shape and maximum position can be introduced, further improving the fit with experimental data.

mostly by the energetic structure of the interface between semiconductor and insulator as well as by interface states formed there which are usually difficult to study. It is likely that these interface states are responsible for markedly different behaviour of the Se–TNB system with respect to the others studied, and for this reason the Se–TNB case will be discussed separately.

Photoinjection of electrons into TNB from amorphous selenium indicates that the transport states in the sensitizer and insulator exhibit a good match for this process, while the injection of holes is

inhibited by a relatively large energy barrier. We have ruled out the possibility that this asymmetry in photoinjection is caused by difference between hole and electron mobilities because mobilities of electrons and holes in TNB are almost equal as results from.[1]

Both features, i.e. the steep increase of the photocurrent and the strange behaviour of $G(\lambda)$ function as presented in Figure 1 and Figure 3 could be understood if one assumes a significant role of carrier traps at or near the interface. Taking into consideration the fact that the number of trapping sites at the interface is limited and that trap-release times are finite, it is easy to predict that under the conditions of steady-state illumination an equilibrium of carrier injection controlled by these traps will result. However, if the source of carriers (the Se bulk) will supply a sufficient number of carriers to "dynamically" fill all surface states then these states will no longer control the injection. The concentration of carriers produced and transported to interface depends on two factors: the applied field and the quantum efficiency of photogeneration process in a-Se, the latter being dependent also on λ and F. According to the above concepts at a critical electric field F_c one should expect a step-like rise of the current (a similar phenomenon is observed in SCL currents in insulators with traps as the so called trap-filled limit). The critical field F_c in our system was of the order of 10^4 V cm and was not due to the space charge limitations of the TNB bulk. A slight increase of F_c with an increase of the incident photon energy can be rationalized as follows: on decreasing the wavelength, the absorption take place closer to the surface of a-Se resulting in a strong increase of the surface recombination, this will reduce the number of carriers being able to reach the interface. Then a larger external field is necessary to again supply enough carriers from the generation region to refill remaining empty traps and thus reach the state of dynamically filled interface traps. No critical field can be found for photon energy below 2.13 eV (2.13 eV being the value of the energy gap in a-Se[15]), probably due to strong decrease of η_e^{Se} which results in the fact that the generation region cannot further supply enough carriers to obtain filling of all present surface states.

Let us now return to the analysis of the wavelength dependence of the parameter $G(\lambda)$ (see Figure 3). Generally $G(\lambda)$ is of the order of 10^{-5}–10^{-3} and is wavelength-dependent with the maximum occurring at ca. 570 nm (2.17 eV), i.e. surprisingly close to the energy gap in a-Se. The rise of $G(\lambda)$ between 620 nm and 570 nm results probably from the fact that due to weak absorption in that range carriers are generated everywhere in the selenium bulk, thus causing a certain

number of carriers to be injected into TNB in their "hot state" i.e. prior to thermalization. Such a possibility does not exist in the regions of strong absorption. An apparent decrease of $G(\lambda)$ for photons carrying energy higher than E_g of a-Se has probably two reasons: (i) The residual trapped charge at the interface should rise together with photon energy and the photogeneration efficiency. This trapped charge will decrease the effective electric field in the sensitizer layer and thus the efficiency of photogeneration and subsequent injection. (ii) Due to the generation taking place close to the a-Se surface, all carriers have to pass through the sensitizer's thickness as well as through the interface and are subjected to all possible processes of carrier loss.

Considering the ability of electrodes used in our experiments to inject or photoinject charge carriers into the insulator, one can estimate positions of its valence and conduction bands providing the positions of the electrode levels are known.

It is known from the literature that the gas-phase electron affinity of TNB is 1.86 eV and its ionization potential I_g is 7.4 eV.[16] In crystalline

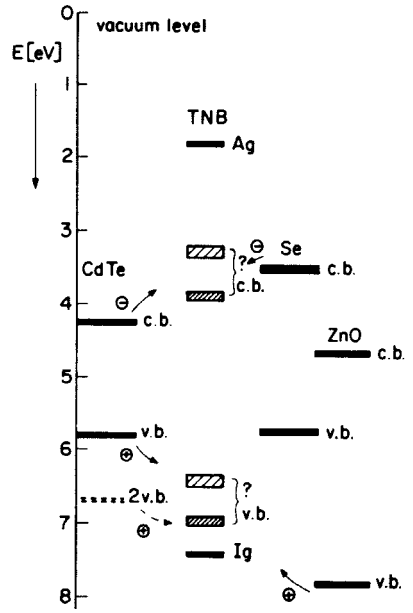

FIGURE 11 Energy level diagram of semiconductor-TNB structure. The values of surface parameters for ZnO and CdTe has been taken from[18] and for a-Se from.[19] The arrows represent observed by photoinjection or dark injection processes. Possible positions of TNB transport states are marked.

TNB, transport states (conduction and valence bands) should be positioned somewhere between these values, diminished or increased, respectively, by the value of the polarization energy of an electron P_- and a hole P_+. These values are not necessarily equal but in a typical molecular crystals are of the order of 1 eV. Taking the literature data about positions of conduction and valence bands of semiconductors used and placing them together on the energy scale we have obtained a scheme (see Figure 11) of possible processes which may be involved in injection into TNB. The most probable positions of TNB transport states are also marked. However, we do not consider the influence of surface states on injection or energy level bending near the surface (sometimes as much as 0.5 eV[17]).

Acknowledgment

The authors wish to acknowledge very useful discussions with Professor J. Sworakowski and Dr. M. Samoç which provided valuable consultation in many aspects of the work. They also wish to thank Dr. J. B. Webb for the preparation of the ZnO films.

References

1. A. Miniewicz, M. Samoc, J. Sworakowski, D. F. Williams and Z. Zboinski, *Mol. Cryst. Liq. Cryst.*, In Press.
2. J. Gonzales-Basurto, F. Sanchez-Sinencio and J. S. Helman, *Phys. Rev.*, **B6**, 3865 (1972).
3. E. Lopez-Cruz, F. Sanchez-Sinencio, A. Rose and J. S. Helman, *Phys. Rev.*, **B22**, 2855 (1980).
4. J. Mort, *Phys. Rev.*, **B5**, 3329 (1972).
5. W. R. Salaneck and E. L. Lind, *J. Appl. Phys.*, **43**, 481 (1972).
6. J. Mort and R. L. Emerald, *J. Appl. Phys.*, **45**, 175 (1973).
7. R. L. Emerald and J. Mort, *J. Appl. Phys.*, **45**, 3943 (1974).
8. P. Ng, J. B. Webb and D. E. Brodie, *Can. J. Phys.*, **54**, 446 (1976).
9. J. C. Knights and E. A. Davis, *J. Phys. Chem. Solids*, **35**, 543 (1974).
10. D. M. Pai and R. C. Enck, *Phys. Rev.*, **B11**, 5163 (1975).
11. J. Stuke and H. Keller, *Phys. Stat. Sol.*, **7**, 189 (1964).
12. T. H. Myers, S. W. Edwards and J. F. Schetzina, *J. Appl. Phys.*, **52**, 4231 (1981).
13. B. Reimer and H. Baessler, *Phys. Stat. Sol.*, **a32**, 435 (1975).
14. J. Godlewski and J. Kalinowski, *Phys. Stat. Sol.*, **a53**, 161 (1979).
15. J. Mort and H. Scher, *Phys. Rev.*, **B3**, 334 (1971).
16. H. Meier, "Organic Semiconductors"/Monographs in Modern Chemistry, vol. 2, Verlag Chemie (1974).
17. A. J. Twarowski, *J. Chem. Phys.*, **77**, 1458 (1982).
18. R. K. Swank, *Phys. Rev.*, **153**, 844 (1967).
19. J. Mort and A. I. Lakatos, *J. Non-Cryst. Sol.*, **4**, 117 (1970).